Research Square

Preprints are preliminary reports that have not undergone peer review.
They should not be considered conclusive, used to inform clinical practice,
or referenced by the media as validated information.

Daidzein Attenuates Busulfan-Induced Premature Ovarian Insufficiency Through Coordinated Modulation of Redox Homeostasis, Inflammatory and Apoptotic Signaling: A Comparative animal Study

Fatemeh Rahimi
Shiraz University of Medical Sciences
Farhad Koohpeyma
Shiraz University of Medical Sciences
Fatemeh Khademi
Shiraz University of Medical Sciences
Sanaz Alaee
Shiraz University of Medical Sciences
Fatemeh Asadian
Shiraz University of Medical Sciences
Naeimehossadat Asmarian
Shiraz University of Medical Sciences
Fatemeh Zal
fatemehzal@yahoo.com

Shiraz University of Medical Sciences

Research Article

Keywords: Daidzein, Busulfan, Premature Ovarian insufficiency, Nrf2, FOXL2, Oxidative Stress, Stereology, Phytoestrogen

Posted Date: November 19th, 2026

DOI: https://doi.org/10.21203/rs.3.rs-11246461/v1

License: This work is licensed under a Creative Commons Attribution 4.0 International License.
Read Full License

Additional Declarations: No competing interests reported.

Daidzein Attenuates Busulfan-Induced Premature Ovarian Insufficiency Through Coordinated Modulation of Redox Homeostasis, Inflammatory and Apoptotic Signaling: A Comparative animal Study

Fatemeh Rahimi[1], Farhad Koohpeyma[2,3], Fatemeh Khademi[1], Sanaz Alaee[4], Fatemeh Asadian[5], Naeimehossadat Asmarian[6], Fatemeh Zal [1,7*]

[1.]Department of Biochemistry, School of Medicine, Shiraz University of Medical Sciences, Shiraz, Iran.

[2.] Endocrinology and Metabolism Research Center, Shiraz University of Medical Sciences, Shiraz, Iran.

[3.] Student research committee, Shiraz University of Medical Sciences, Shiraz, Iran

[4.] Reproductive Biology Department, School of Advanced Medical Sciences and Technologies, Shiraz University of Medical Sciences, Shiraz, Iran.

[5.]Diagnostic Laboratory Sciences and Technology Research Center, School of Paramedical Sciences, Shiraz University of Medical Sciences, Meshkinfam Street, Shiraz, Iran.

[6.]Anesthesiology and Critical Care Research Center, Shiraz University of Medical Sciences, Shiraz, Iran.

[7.]Infertility Research Centre, Shiraz University of Medical Sciences, Shiraz, Iran.

***Corresponding author:** Fatemeh Zal. Department of Biochemistry, School of Medicine, Shiraz University of Medical Sciences, Shiraz, Iran, Infertility Research Centre, Shiraz University of Medical Sciences, Shiraz, Iran. Email: fatemehzal@yahoo.com, https://orcid.org/0000-0002-7078-4854

Abstract

Background: Premature ovarian insufficiency (POI) is a major complication of gonadotoxic chemotherapy that impairs fertility and endocrine function. Busulfan induces ovarian injury through oxidative stress, inflammation, and apoptosis. Although daidzein exhibits antioxidant and phytoestrogenic properties, its efficacy relative to estradiol has not been comprehensively evaluated in busulfan-induced POI. This study compared the protective effects of daidzein and estradiol on ovarian structure, function, biomarkers and the expression of core genes involved in the three pathways previously mentioned.

Methods: Thirty female Sprague-Dawley rats were assigned to Control, daidzein, busulfan-induced POI, POI+ daidzein, or POI+estradiol groups (n=6). Treatments continued for 50 days after busulfan administration. The stereological analysis assessed the ovarian morphology and follicle numbers. Oxidative stress biomarkers (SOD, CAT, TAC, and MDA) in ovarian tissue and estradiol, progesterone, TNF-α concentration in serum were measured using commercial kits. Expression of ovarian genes (Nrf2, FOXL2, ERα, ERβ, BCL2, CASP3, and TNF-α*)* was evaluated using Real-Time PCR.

Results: Busulfan significantly reduced ovarian stereological indices, healthy follicle counts, SOD and CAT activity, TAC, estradiol and progesterone concentration, and the expression of Nrf2, FOXL2, ERα, ERβ, and BCL2 *genes*, while increasing atretic follicles, MDA, TNF-α, and CASP3 genes expression ($P<0.05$). Daidzein significantly improved ovarian morphology, follicular preservation, antioxidant status, hormone levels, and the expression of Nrf2, FOXL2, and BCL2 genes, while reducing MDA, TNF-α, and CASP3 gene expression ($P<0.05$). Estradiol improved ovarian morphology, estradiol level, SOD activity, TAC and , the expression of Nrf2, BCL2, and CASP3 genes, while did not significantly affect CAT activity, progesterone level and FOXL2, or TNF-α genes expression.

Conclusion: Daidzein partially protected against busulfan-induced POI by preserving ovarian morphology, endocrine function, antioxidant defenses, and molecular pathways regulating oxidative stress, inflammation, apoptosis, and estrogen signaling. These findings support daidzein as a promising adjunctive strategy for ovarian protection during chemotherapy and warrant further mechanistic and translational investigation.

Keywords: Daidzein; Busulfan; Premature Ovarian insufficiency; Nrf2; FOXL2; Oxidative Stress; Stereology; Phytoestrogen

1. Background:

Primary ovarian insufficiency (POI), previously termed premature ovarian failure, is a heterogeneous reproductive endocrine disorder characterized by cessation of ovarian function before the age of 40 years, manifesting as menstrual disturbances, hypergonadotropic hypogonadism, hypoestrogenism, and impaired fertility[1]. Affecting approximately 1–3.7% of women globally, POI imposes a substantial burden through osteoporosis, cardiovascular disease, metabolic dysfunction, and reduced quality of life and because the molecular mechanisms of follicular depletion are incompletely understood, effective therapies remain limited [1, 2].

Despite improvements in chemotherapy agents and reduction in their side effects, chemotherapy is still a clinically significant cause of POI, in young cancer survivors [3, 4].Currently, embryo and oocyte cryopreservation are the only well-known options for fertility preservation in women and effective therapies remain limited, as the molecular mechanisms of follicular depletion are incompletely understood [1].Therefore, further studies to identify new, less expensive treatments based on reproductive biology is a necessity.

Alkylating agents such as cyclophosphamide and busulfan are highly gonadotoxic chemotherapy agents due to DNA damage and follicular disruption [5]. For further studies, busulfan- induced ovarian failure is a well-established POI model because reproducibly mimics ovarian changes induced by chemotherapy [5, 6].

In busulfan-induced POI models, ovarian damage arises from the interplay between oxidative stress, inflammation, and apoptosis rather than isolated events. Oxidative stress is a central driver and excessive ROS overwhelms endogenous antioxidant defenses, causing oxidative damage to lipids, proteins, and mitochondrial components, thereby compromising follicular integrity [7]. Nuclear factor erythroid 2-related factor 2 (Nrf2) is a master transcription factor coordinating antioxidant and cytoprotective gene expression and impaired Nrf2 signaling is consistently linked to oxidative damage, granulosa cell apoptosis, and follicular loss in POI models [7, 8]. In addition, forkhead box L2 (FOXL2) is an ovary-specific transcription factor essential for granulosa cell differentiation, follicular maintenance, steroidogenesis and also enhances cellular resistance to oxidative injury by regulating antioxidant and survival genes. Reduced FOXL2 expression is associated with granulosa cell dysfunction, apoptosis, and POI [9, 10]. Therefore, pharmacological Nrf2 and FOXL2 activation represents a promising strategy to counteract oxidative injury and preserve ovarian function during gonadotoxic chemotherapy. As a consequence, oxidative stress, activates NF-κB and increases TNF-α expression, which amplifies inflammation, impairs steroidogenesis, and promotes apoptosis [7, 11, 12]. Mitochondrial apoptosis is regulated by the BCL-2 family; oxidative stress shifts the balance toward pro-apoptotic signaling, facilitating cytochrome c release, caspase activation, and CASP3 cleavage [7, 11, 13]. These interconnected events drive follicular atresia, granulosa cell death and ovarian reserve depletion, highlighting oxidative stress and mitochondrial apoptosis as key therapeutic targets.

Ovarian function also depends on estrogen signaling via ERα and ERβ, both essential for follicular development, steroidogenesis, and fertility. ERβ is the dominant receptor in ovarian tissue, regulating folliculogenesis and granulosa cell function, whereas ERα contributes to systemic endocrine regulation. Disruption of estrogen receptor signaling—whether by aging or chemotherapy—impairs follicular maturation and accelerates follicular atresia, underscoring the importance of preserving estrogen receptor activity as a therapeutic objective [14, 15].

Given the multifactorial nature of chemotherapy-induced ovarian damage, interest has grown in bioactive compounds that modulate multiple pathways. Daidzein, a phytoestrogenic soy isoflavone structurally similar to 17β-estradiol, exhibits its effects through preferential ERβ interaction and estrogen signaling. Studies in diverse models show daidzein has a wide range of pharmacological effects, including antioxidant and anti-inflammatory and also preserves mitochondrial function and limits mitochondrial apoptosis [16, 17] [17, 18]. However, its specific efficacy against busulfan-induced ovarian failure—and its comparative effectiveness relative to estradiol—has not been systematically investigated.

Accordingly, the present study was designed to investigate the protective effects of daidzein against busulfan-induced premature ovarian insufficiency in rats, with estradiol included as a reference compound to benchmark its efficacy against the current standard of care. We hypothesized that daidzein would attenuate chemotherapy-induced ovarian injury by restoring redox homeostasis, suppressing inflammatory signaling, preserving mitochondrial integrity, and maintaining the molecular pathways that govern follicular survival and endocrine function. To test this hypothesis, in busulfan-induced POI rats we evaluated ovarian histoarchitecture and histopathological alterations, serum reproductive hormone concentrations, oxidative stress biomarkers, and the expression of genes involved in antioxidant defense (Nrf2), inflammation (TNF-α), apoptosis (BCL2 and CASP3), estrogen signaling (ERα and ERβ), and granulosa cell identity (FOXL2), alongside detailed stereological assessment of follicular populations and ovarian reserve. By integrating histopathological, biochemical, endocrine, and molecular analyses, this study provides a comprehensive evaluation of the mechanisms through which daidzein mitigates chemotherapy-induced ovarian injury and offers preclinical evidence supporting its potential as a therapeutic strategy for preserving ovarian function following gonadotoxic chemotherapy.

2. Material and methods

2.1. Experimental animals

Thirty adult female Sprague-Dawley rats (weighing 200 ± 20 g, 8–10 weeks old) were obtained from the laboratory animal facility of the Endocrinology and Metabolism Research Center, Shiraz University of Medical Sciences. Animals were housed individually in standard polypropylene cages under controlled environmental conditions (22 ± 2°C, 55 ± 5% humidity) with a 12:12 h light-dark cycle (lights on at 07:00). All animals had free access to standard rodent chow (Behparvar, Tehran, Iran) and tap water ad libitum throughout the experimental period. Sample size was determined using the resource equation method (E = N - k, where E = 10–20), yielding 6

animals per group to achieve adequate statistical power with a significance level of $\alpha = 0.05$ and power of 80%.

All experimental procedures were approved by the Research Ethics Committee of Shiraz University of Medical Sciences (IR.SUMS.AEC.1402.074) and performed in accordance with the guidelines of the National Institutes of Health for the care and use of laboratory animals. Animal care and reporting followed the ARRIVE guidelines [19].

2.2 Induction of Premature Ovarian insufficiency

Estrous cycles were monitored daily by vaginal smear examination for 10 consecutive days prior to the experiment, and only animals exhibiting at least two consecutive regular 4-day estrous cycles were included. Chemotherapy-induced POI was established by a single intraperitoneal injection of busulfan (Sigma-Aldrich, St. Louis, MO, USA) at a dose of 36 mg/kg, administered on the day of estrus (defined by the predominance of cornified epithelial cells), as previously described [20]. To confirm successful POI induction, one randomly selected busulfan-treated animal was euthanized 4 weeks after busulfan administration, and ovarian tissue was examined histopathologically by an experienced pathologist blinded to the experimental groups.

2.3 Experimental Groups and Treatment Protocol

Following confirmation of POI induction, the remaining animals were randomly assigned to five groups (n = 6 per group):

Control: Healthy animals receiving vehicle (normal saline, 1 mL/kg/day, oral gavage)

Daidzein (DZD): Healthy animals receiving daidzein (50 mg/kg/day, oral gavage)[21]

POI: POI animals receiving vehicle (normal saline, 1 mL/kg/day, oral gavage)

POI + DZD: POI animals receiving daidzein (50 mg/kg/day, oral gavage)

POI + Estr: POI animals receiving estradiol (10 µg/kg/day, subcutaneous injection)[22].

Daidzein (Sigma-Aldrich) was dissolved in normal saline and administered daily by oral gavage. Estradiol (Sigma-Aldrich) was dissolved in sesame oil and administered daily by subcutaneous injection. All treatments were initiated one weeks after busulfan administration and continued for 50 consecutive days.

2.4 Tissue Collection and Processing

At the end of the treatment period, animals were deeply anesthetized with an intraperitoneal injection of ketamine (100 mg/kg; Alfasan, Woerden, Netherlands) and xylazine (10 mg/kg; Alfasan, Woerden, Netherlands). Blood samples were collected via cardiac puncture under deep anesthesia immediately after confirming the absence of pedal reflex, and prior to euthanasia to avoid hypoxia-induced alterations in biochemical parameters. Blood samples were centrifuged at 3500 rpm for 10 minutes at 4°C, and serum was separated and stored at -80°C until analysis.

Following blood collection, animals underwent necropsy. The right ovary from each animal was immediately fixed in 4% buffered formalin for histopathological and stereological evaluations. The left ovary was rapidly excised, snap-frozen in liquid nitrogen, and stored at -80°C for subsequent molecular and biochemical analyses. Specifically, from each group, the left ovaries of 3 randomly selected animals were used for gene expression analysis, and the left ovaries of the remaining 3 animals were used for antioxidant enzyme activity assays. Finally, animals were euthanized by CO_2 inhalation in accordance with institutional ethical guidelines, after blood collection and tissue harvesting were completed.

2.5 Measurement of oxidative stress biomarkers in ovarian tissue

For biochemical assessments, ovarian tissue samples were homogenized in ice-cold phosphate-buffered saline (PBS) and centrifuged at 12,000 × g for 15 minutes at 4°C. The resulting supernatants were collected and used for the colorimetric determination of total antioxidant capacity (TAC), malondialdehyde (MDA) levels, and the enzymatic activities of catalase (CAT) and superoxide dismutase (SOD), using commercial kits (Karmania Pars Gene Company, Kerman, Iran) according to the manufacturer's instructions. TAC was measured using the cupric reducing antioxidant capacity method, and the absorbance was read at 450 nm. MDA levels were determined based on its reaction with thiobarbituric acid (TBA) to form a colored complex, with absorbance measured at 532 nm. Catalase activity was assessed using the Purpald method, in which formaldehyde produced from methanol oxidation reacts with Purpald to generate a chromophore measured at 540 nm. SOD activity was evaluated using the WST-1 method, which measures the inhibition of nitroblue tetrazolium (NBT) reduction by superoxide radicals; the absorbance was read at 570 nm. All samples were run in duplicate, and the activities of CAT and SOD were normalized to total protein content, which was determined using the Bradford method.

2.6 Measurement of serum TNF-α and reproductive hormone levels

Serum concentrations of tumor necrosis factor-alpha (TNF-α), estradiol (E2), and progesterone (PROG) were measured using commercially available enzyme-linked immunosorbent assay (ELISA) kits (BT LAB, China) according to the manufacturer's instructions. The TNF-α levels were determined using a sandwich ELISA kit (Cat. No. E0764Ra) with a standard curve range of 5–1000 ng/L and a sensitivity of 2.51 ng/L. Estradiol and progesterone were measured using competitive ELISA kits (Cat. No. EA0011Ra and EA0063Ra, respectively), with standard curve ranges of 15–3000 ng/L and 0.2–60 ng/mL, and sensitivities of 8.11 ng/L and 0.096 ng/mL, respectively. All samples were assayed in duplicate. The intra-assay and inter-assay coefficients of variation (CVs) for all kits were < 10% and < 12%, respectively. Serum samples were diluted as necessary according to the manufacturer's recommendations (2–5 fold for E2 and PROG), and the optical density of each well was read at 450 nm using a microplate reader. Finally, the concentrations were calculated from standard curves generated with each assay.

2.7 RNA isolation and quantitative RT-PCR for gene expression analysis

Total RNA was extracted from ovarian tissue samples using RNA BIOZOL isolation reagent according to the manufacturer's instructions. The concentration and purity of extracted RNA were determined spectrophotometrically at 260/280 nm, and RNA integrity was confirmed by agarose gel electrophoresis. Complementary DNA (cDNA) was synthesized from 1 µg of total RNA using the QuantiTect Reverse Transcription Kit (SinaClon, Iran) in a 20 µL reaction volume, following the manufacturer's protocol. Quantitative real-time PCR (qRT-PCR) was performed using the ABI 7500 Real-Time PCR System (Applied Biosystems Inc., Foster City, CA, USA) with SYBR Green Master Mix (Applied Biosystems). The mRNA expression levels of Nrf2, TNF-α, BCL2, CASP3, ERα (Esr1), ERβ (Esr2), and FOXL2 were quantified. The specific primer sequences are listed in Table 1. All reactions were run in duplicate, and non-template controls were included to verify the absence of contamination. Melting curve analysis and standard curve slopes were assessed to confirm product specificity and amplification efficiency. The relative expression of each target gene was calculated using the $2^{-\Delta\Delta Ct}$ method, with β-actin as the internal reference gene for normalization. The qRT-PCR cycling conditions consisted of an initial denaturation at 95°C for 10 minutes, followed by 40 cycles of 95°C for 15 seconds and 60°C for 1 minute. A dissociation step was included at the end of each run to generate melting curves for specificity verification. The amplification efficiency for each primer pair ranged between 90–110%, and the correlation coefficient (R^2) of the standard curves was > 0.99.

Table 1. The sequence of designed primers.

Gene	Forward Primer (5' → 3')	Reverse Primer (5' → 3')
Nrf2	TGA TTT AAG CAG CAT	GTA TTA AGA CAC TGT AAC TCG GG
TNF-α	CCC ACG TCG TAG TAG CAA ACC AC	TAG GGC AAG GGC TCT TGA TG
BCL2	CCT GGT GGA CAA CAT CGCT	TCG CTA CAA CAG GTG GTC C
CASP3	GAGCTGGACTGCGGTATTGAG	AACCATGACCCGTCCCTTGA
***ERα* (Esr1)**	CCA AAG CCT CGG GAA TGG	AGC TGC GGG CGA TTG AG
***ERβ* (Esr2)**	TCA GGC ACA TCA GTA ACA AG	CAG CAG CAG GTC ATA CAC
FOXL2	TCT TCC AGG TCG GTG GAC TCA	TTC CGT TCT CAG GCA GTG TG
β-actin	AAG GCC AAC CGT GAA AAG AT	ACC AGA GGC ATA CAG GGA C

2.8. Tissue preparation and stereological analysis

At the end of the treatment period, the rats were weighed using a digital scale (A&D, Japan, with 0.1 g precision), deeply anesthetized with ketamine/xylazine (Alfasan, Netherlands), and the right ovaries were surgically removed. The ovaries were immediately weighed using a three-decimal precision balance and fixed in 4% buffered formalin for 48 hours. After routine tissue processing, the samples were embedded in cylindrical paraffin blocks. The orientator method was employed to obtain isotropic uniform random (IUR) sections [23]. Consecutive 5- and 20-µm-thick sections were then cut using a microtome and stained with hematoxylin and eosin (H&E; Merck, Germany) for stereological evaluations.

2.9. Estimation of ovarian volume

The total volume of the ovary was estimated using the Cavalieri principle on 8–12 systematic random sections. A point-counting grid was superimposed on the images, and the number of points hitting the ovarian sections was counted. The ovarian volume was calculated using the following formula [24]:

$$V_{total\ ovary=} \sum_{i=1}^{n} p \times a(p) \times t$$

Where $\sum_{i=1}^{n} p$ is the total number of points superimpose on the image, a(p) is the area associated with each point, and t is the distance between the sample sections. The same formula can be used to calculate the volume of the cortex, medulla, and corpus luteum, provided that the total number of points hitting each individual structure (cortex, medulla, and corpus luteum) is substituted separately into the equation.

2.11 Estimation of follicle numbers

The total number of follicles was estimated using the optical disector method on 20-µm-thick sections. Follicles were classified as primordial, preantral (unilaminar & multilaminar), antral, Graafian, and atretic based on previously established criteria (24,25). The numerical density of follicles was calculated using the following formula:

$$Nv = \frac{\sum_{i=1}^{n} Q}{\sum_{i=1}^{n} P \times h \times (\frac{a}{f})} \times \frac{t}{BA}$$

Where "$\sum_{i=1}^{n} Q$" was the number of the follicles counted in all the Disectors, "h" was the height of the optical Disector, "a/f" was the area of the counting frame, "$\sum_{i=1}^{n} P$" was the total number of the counted frames, "BA" or block advance was the setting of the microtome to cut the paraffin block, and "t" was the mean of the final section thickness[24]. To estimate the total number of the follicles, the following formula was applied:

$$N_{(Follicles)} = N_{V\ (follicles/ovary)} \times V_{(ovary)}$$

2.12. Statistical Analysis

SPSS 23 (SPSS Inc., Chicago, USA) was used for analysis. Data were first tested for normality using the Shapiro-Wilk test. Data exhibited a normal distribution and variance homogeneity; thus, parametric tests were done. A one-way ANOVA was performed to compare five research groups' means. Next, LSD post-hoc test determined significant differences. Statistical significance was considered at $p<0.05$. Graphical representations were produced using GraphPad Prism Software version 9.5.0. Data is presented as Mean ± SD. Heatmap analysis was performed using R software (version 4.6.0) with the 'pheatmap' package. Data were standardized using Z-score transformation prior to

hierarchical clustering with Euclidean distance and Ward's linkage method. Group separators were added to visualize the distinct experimental groups.

3. Results

3.1 Oxidative stress and inflammatory biomarkers

The mean activities of superoxide dismutase (SOD), catalase, and total antioxidant capacity (TAC) were significantly lower in the POI group than in the Control and DZD groups ($P<0.001$; Figure 1A-C). SOD activity was significantly increased in both the POI+DZD and POI+Estr groups compared with the POI group ($P<0.001$). However, SOD activity remained significantly lower than that observed in the Control and DZD groups ($P\leq0.001$; Figure 1A).

Catalase activity was significantly increased in the POI+DZD and POI+Estr groups compared with the POI group ($P=0.002$; $P=0.009$ respectively), whereas no significant difference was observed between the POI+Estr and POI+DZD groups. Nevertheless, catalase activity remained significantly lower in the POI+DZD and POI+Estr groups than in the Control group ($P=0.002$ and $P=0.001$, respectively; Figure 1B).

TAC was significantly increased in both the POI+DZD and POI+Estr groups compared with the POI group ($P<0.001$). Despite this improvement, TAC remained significantly lower in the POI+DZD and POI+Estr groups than in the Control group ($P=0.001$; $P=0.017$ respectively). TAC was also significantly lower in the POI+DZD and POI+Estr groups than in the DZD group ($P<0.001$ and $P=0.001$, respectively; Figure 1C).

The mean concentrations of TNF-α and malondialdehyde (MDA) were significantly higher in the POI group than in the Control and DZD groups ($P<0.001$; Figure 3D, E). MDA levels were significantly reduced in both the POI+DZD and POI+Estr groups compared with the POI group ($P<0.001$). In addition, TNF-α concentration remained significantly higher in the POI+Estr group than in the DZD and POI+DZD group ($P=0.001$; $P=0.042$ respectively; Figure 1D, E).

3.2. Serum hormone concentrations

Progesterone and estrogen concentrations were significantly reduced in the POI group compared with the Control group ($P=0.020$ and $P=0.003$, respectively) and the DZD group ($P<0.001$ and $P=0.024$, respectively; Figure 1F, G). Progesterone concentration was significantly higher in the DZD group than in the Control group ($P=0.013$). The POI+DZD group showed a significant increase in progesterone concentration compared with the POI group ($P=0.034$), whereas no significant difference was observed between the POI+Estr and POI groups. Progesterone concentration remained significantly lower in the POI+DZD and POI+Estr groups than in the DZD group ($P=0.007$ and $P<0.001$, respectively).

Estrogen concentration was significantly increased in both the POI+DZD and POI+Estr groups compared with the POI group ($P=0.012$ and $P=0.015$, respectively; Figure 1G).

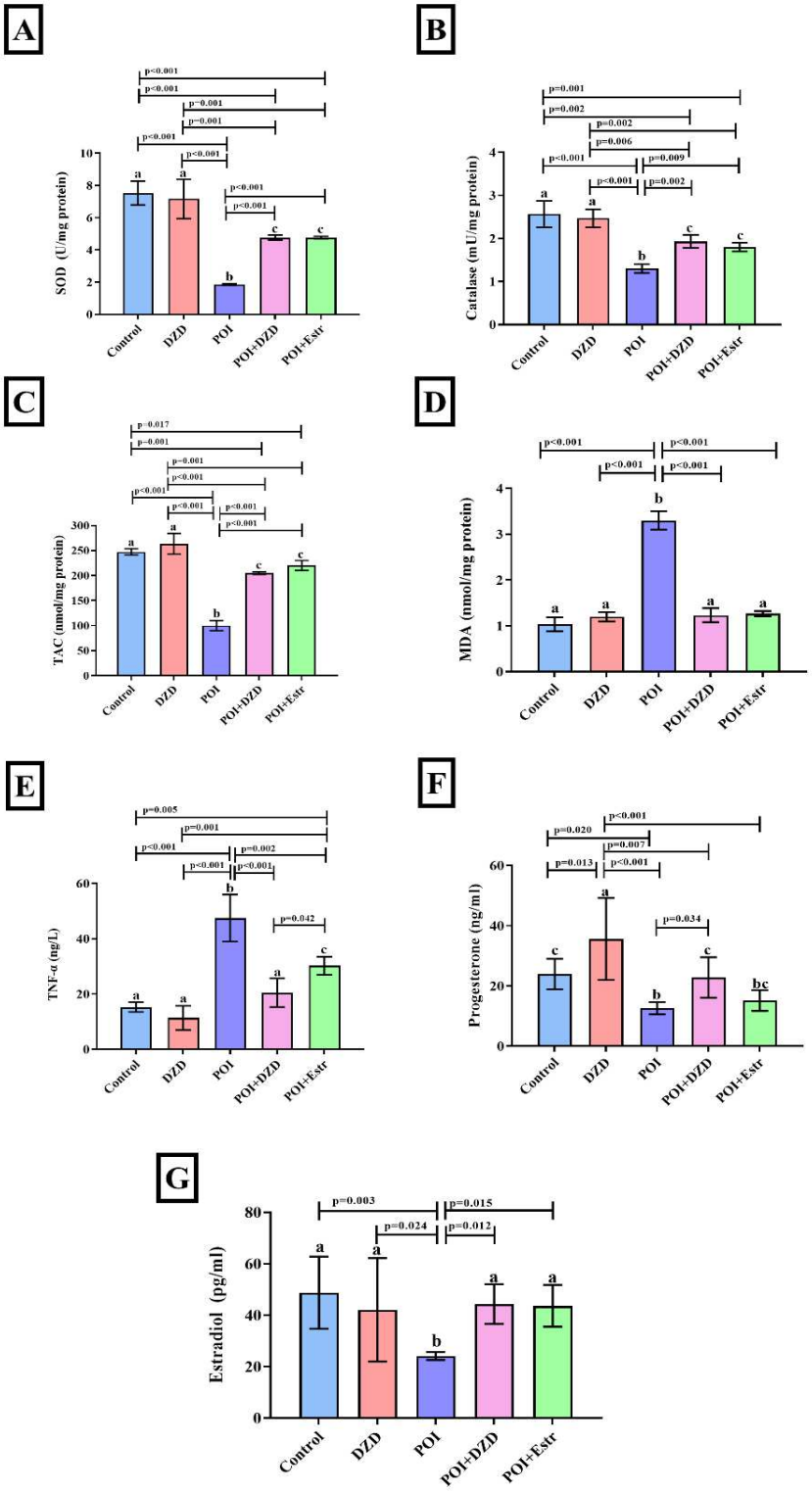


Figure 1. Daidzein ameliorates oxidative stress, inflammatory responses, and hormonal disturbances in rats with busulfan-induced premature ovarian insufficiency. (A) Superoxide dismutase (SOD) activity, (B) catalase activity, (C) total antioxidant capacity (TAC), (D) malondialdehyde (MDA)

concentration, (E) tumor necrosis factor-α (TNF-α) concentration, (F) serum progesterone concentration, and (G) serum estradiol concentration. Experimental groups included the healthy control (Control), healthy rats treated with daidzein (DZD), busulfan-induced premature ovarian insufficiency (POI), POI treated with daidzein (POI+DZD), and POI treated with estradiol (POI+Estr). Data are presented as **mean ± SD**. Statistical comparisons were performed using **one-way analysis of variance (ANOVA)** followed by the **least significant difference (LSD) post hoc test**. Exact *P* values are indicated above the corresponding comparisons. Different lowercase letters above the bars denote statistically significant differences among groups ($P < 0.05$), whereas groups sharing at least one common letter are not significantly different.

3.3. Gene expression analysis

As depicted in Figure 2A, TNF-α expression was significantly upregulated in the POI group versus the Control and DZD groups (P = 0.001), an effect that was significantly attenuated by DZD co-treatment (P = 0.006). Notably, the POI+Estr group also showed significantly higher TNF-α levels than the Control and DZD groups (P = 0.027 and P = 0.016, respectively).

Nrf2 gene expression was significantly decreased in the POI group compared with the Control and DZD groups (P=0.005 and P<0.001, respectively; Figure 2B). The DZD group exhibited significantly higher Nrf2 expression than the Control, POI+DZD, and POI+Estr groups (all P<0.001). Compared with the POI group, Nrf2 expression was significantly increased in the POI+DZD and POI+Estr groups (P=0.002 and P=0.007, respectively).

FOXL2 expression was significantly reduced in the POI group compared with the Control and DZD groups (P<0.001; Figure 2C). FOXL2 expression was significantly increased in the POI+DZD group compared with the POI group (P=0.002). In contrast, FOXL2 expression remained significantly lower in the POI+Estr group than in the Control and DZD groups (P=0.015 and P=0.021, respectively).

ERα expression was significantly lower in the DZD, POI, POI+DZD, and POI+Estr groups than in the Control group (P=0.002, P<0.001, P<0.001, and P<0.001, respectively; Figure 2D). No other significant intergroup differences were observed.

ERβ expression was significantly lower in the Control, POI, POI+DZD, and POI+Estr groups than in the DZD group (P=0.004, P=0.003, P=0.028, and P=0.003, respectively; Figure 2E). No additional significant differences were detected among the remaining groups.

BCL-2 expression was significantly higher in the Control, DZD, POI+DZD, and POI+Estr groups than in the POI group (P=0.014, P=0.004, P=0.012, and P=0.011, respectively; Figure 2F). Caspase-3 expression was significantly lower in the Control, DZD, POI+DZD, and POI+Estr groups than in the POI group (P<0.001, P<0.001, P=0.001, and P=0.001, respectively; Figure 2G). No other significant differences were observed for either gene.

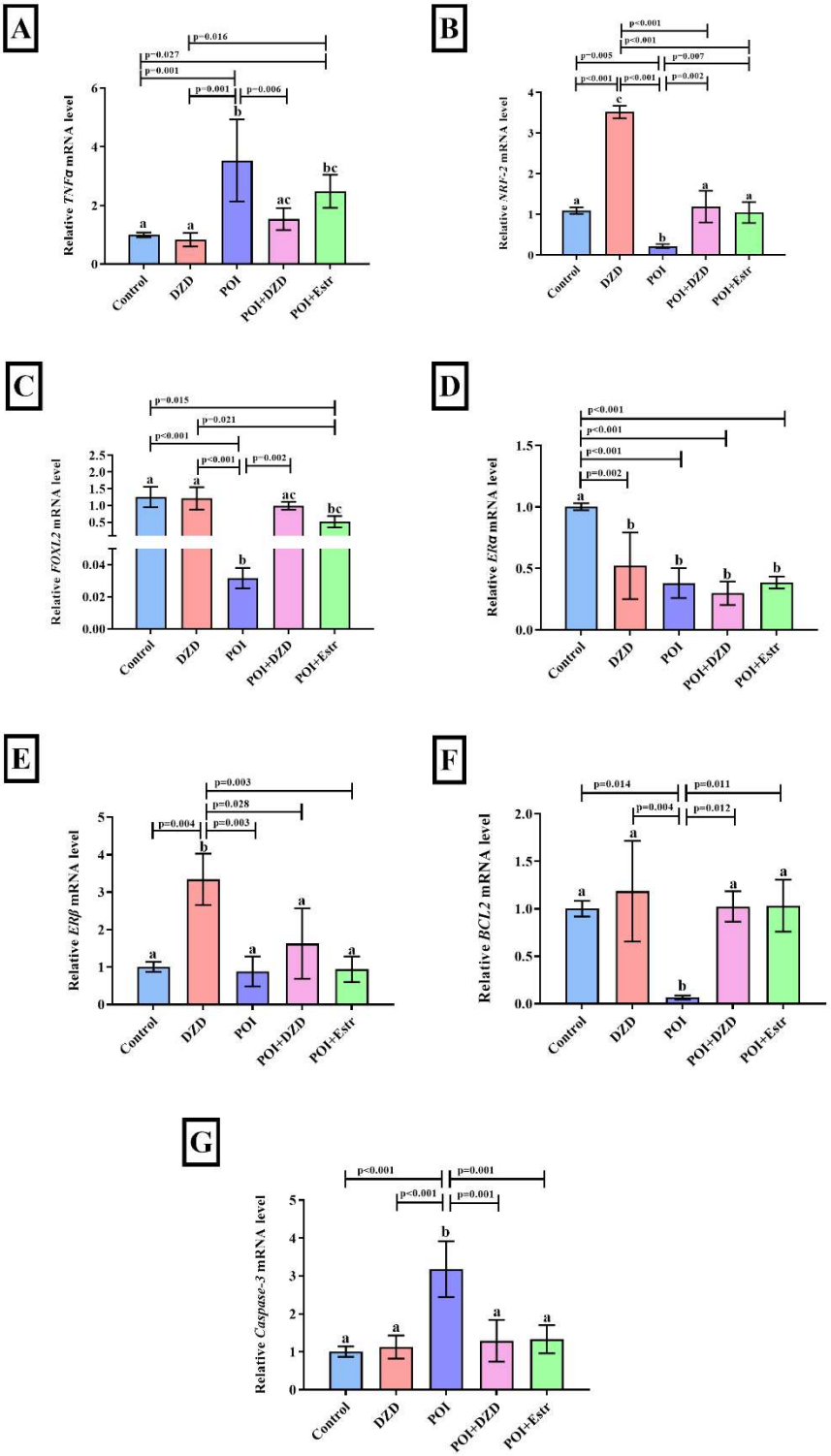


Figure 2. Daidzein modulates ovarian expression of genes associated with inflammation, antioxidant defense, estrogen signaling, and apoptosis following busulfan-induced premature ovarian insufficiency. Relative ovarian mRNA expression of TNF-α, Nrf2, FOXL2, ESR1 (ERα), ESR2 (ERβ), BCL2, and Caspase-3 in Control, DZD, POI, POI+DZD, and POI+Estr groups. Transcript

levels were determined by qRT-PCR and expressed relative to the internal control gene using the $2^{-\Delta\Delta Ct}$ method. Values are presented as mean ± SD. Statistical significance was determined by one-way ANOVA followed by the LSD post hoc test. Exact P values are shown above the relevant comparisons. Different lowercase letters denote significant differences ($P < 0.05$).

3.4 Body weight and ovarian stereology

Body weight was significantly lower in the POI group than in the Control and DZD groups (P=0.040 and P=0.002, respectively; Figure 3A). Body weight was significantly increased in the POI+DZD group compared with the POI group (P=0.008), whereas no significant difference was observed between the POI+Estr and POI groups. However, body weight remained significantly lower in the POI+Estr group than in the DZD group (P=0.020).

Ovarian weight and volume, cortical volume, medullary volume, and corpus luteum volume were all significantly reduced in the POI group compared with the Control and DZD groups (P<0.05). These parameters were significantly increased in both the POI+DZD and POI+Estr groups compared with the POI group (P<0.05). Despite this improvement, corpus luteum volume remained significantly lower in the POI+DZD group than in the Control and DZD groups (P=0.014 and P=0.036, respectively) and in the POI+Estr group than in the Control and DZD groups (P=0.008 and P=0.022, respectively; Figure 3F).

3.5 Follicular assessment

The numbers of primordial, preantral, antral, and Graafian follicles were significantly reduced, whereas the number of atretic follicles was significantly increased, in the POI group compared with the Control and DZD groups (P<0.001; Figure 3G-K).

Neither the POI+DZD nor the POI+Estr group showed a significant change in primordial follicle number compared with the POI group; however, both groups had significantly fewer primordial follicles than the Control (P=0.007 and P<0.001, respectively) and DZD groups (P=0.006 and P<0.001, respectively; Figure 3G).

Preantral follicle number was significantly increased in the POI+DZD and POI+Estr groups compared with the POI group (P=0.020 and P=0.005, respectively). However, the POI+DZD group had significantly fewer preantral follicles than the DZD group (P=0.041; Figure 3H).

Both the POI+DZD and POI+Estr groups exhibited significantly higher numbers of antral and Graafian follicles than the POI group (P<0.05; Figure 3I, J). Nevertheless, the number of Graafian follicles remained significantly lower in the POI+DZD group than in the Control and DZD groups (P=0.027 and P=0.013, respectively; Figure 3J).

The number of atretic follicles was significantly reduced in both the POI+DZD and POI+Estr groups compared with the POI group (P<0.001). However, atretic follicle number remained significantly higher in the POI+DZD and POI+Estr groups than in the Control and DZD groups (P=0.006 and P=0.006, and P=0.008 and P=0.007, respectively; Figure 3K).

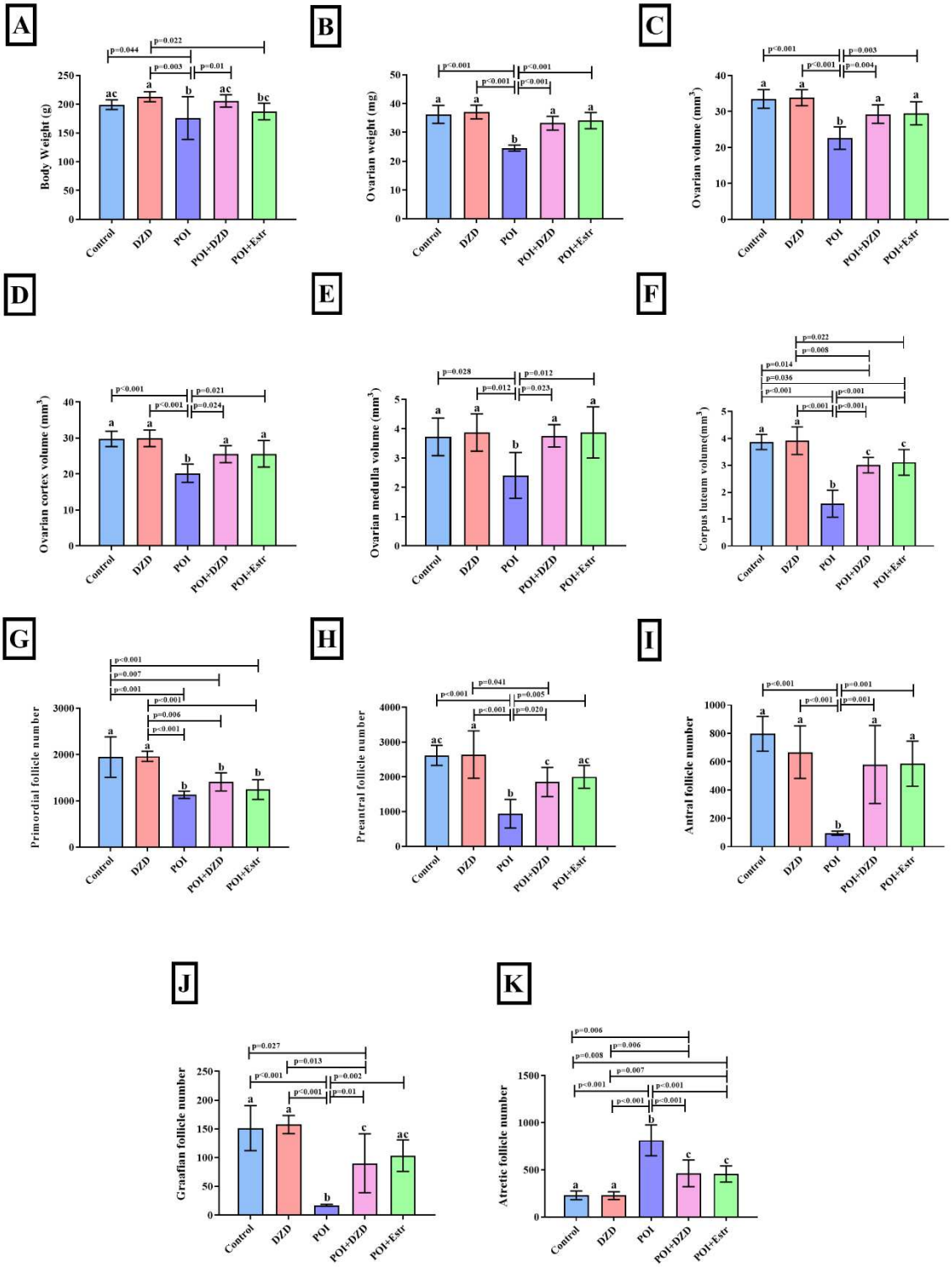


Figure 3. Effects of daidzein on body weight, ovarian stereological parameters, and follicular populations in a busulfan-induced premature ovarian insufficiency rat model. (A) Body weight, (B) ovarian weight, (C) total ovarian volume, (D) ovarian cortex volume, (E) ovarian medulla volume, (F) corpus luteum volume, (G) primordial follicle number, (H) preantral follicle number, (I) antral follicle

number, (J) Graafian follicle number, and (K) atretic follicle number. Experimental groups included the healthy control (Control), healthy rats treated with daidzein (DZD), busulfan-induced premature ovarian insufficiency (POI), POI treated with daidzein (POI+DZD), and POI treated with estradiol (POI+Estr). Data are presented as **mean ± SD**. Statistical analyses were performed using **one-way analysis of variance (ANOVA)** followed by the **least significant difference (LSD) post hoc test**. Exact *P* values are shown above the corresponding comparisons. Different lowercase letters above the bars indicate statistically significant differences among groups ($P < 0.05$), whereas groups sharing at least one common letter are not significantly different.

3.6. Histopathological Findings of Ovarian Tissue

Histopathological examination of hematoxylin and eosin (H&E)-stained ovarian sections (Figure 4) demonstrated well-preserved ovarian architecture in both the Control (Figures 4A and 4F) and DZD (Figures 4B and 4G) groups. The ovarian cortex contained follicles at different developmental stages, including preantral and secondary follicles, together with numerous well-developed corpora lutea exhibiting normal histological organization, indicative of physiological folliculogenesis and ovulatory activity. The ovarian stroma displayed normal cellular organization without evidence of follicular degeneration or widespread follicular atresia.

In contrast, ovarian sections from the POI group (Figures 4C and 4H) exhibited marked histopathological alterations characterized by a pronounced depletion of developing follicles, a substantial increase in atretic follicles, relative thinning of the cortical region, a marked reduction in the number of corpora lutea, and disruption of the normal ovarian architecture. Higher-magnification examination revealed atretic follicles with disorganization of the granulosa cell layers, collapse of follicular architecture, and degenerative changes within the oocyte, indicating severe impairment of the follicular reserve and folliculogenesis. Collectively, these morphological findings confirm the successful establishment of the busulfan-induced premature ovarian insufficiency (POI) model and demonstrate extensive gonadotoxic injury.

Administration of daidzein following busulfan exposure (Figures 4D and 4I) resulted in a noticeable improvement in ovarian histomorphology. The number of preantral follicles increased, whereas the incidence of follicular atresia was reduced compared with the untreated POI group. Moreover, the structural integrity of the granulosa cell layers and ovarian stroma was largely preserved, accompanied by partial restoration of the follicular reserve. These observations suggest that daidzein attenuated busulfan-induced ovarian injury and improved the preservation of ovarian tissue architecture.

Similarly, ovarian sections from the POI+Estr group (Figures 4E and 4J) demonstrated partial histological recovery. Compared with the untreated POI group, the numbers of secondary and preantral follicles were increased, while follicular atresia was less pronounced. Nevertheless, the abundance of developing follicles and the overall ovarian morphology remained inferior to those observed in the healthy groups, indicating only partial restoration of ovarian structure.

Overall, histopathological evaluation demonstrated that busulfan-induced premature ovarian insufficiency was associated with severe depletion of the follicular reserve, increased follicular

atresia, reduced corpus luteum formation, and disruption of normal ovarian histoarchitecture. Treatment with either daidzein or estradiol ameliorated these pathological alterations by preserving follicular morphology and partially restoring ovarian architecture. Morphological improvement appeared more pronounced in the daidzein-treated group, particularly with respect to follicular preservation and attenuation of follicular atresia.

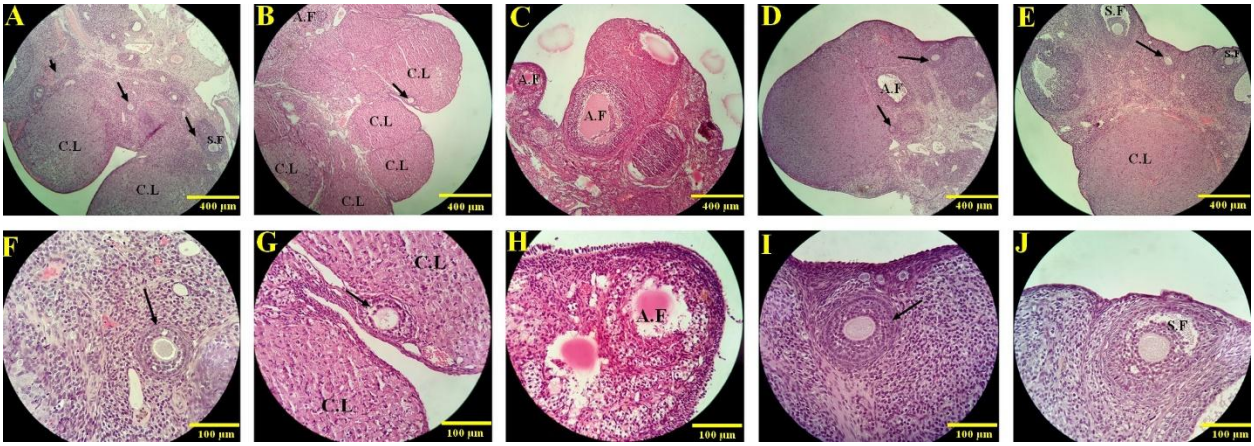


Figure 4. Histopathological evaluation of ovarian tissue in experimental groups following busulfan-induced premature ovarian insufficiency and therapeutic intervention with daidzein or estradiol. Representative hematoxylin and eosin (H&E)-stained ovarian sections from the experimental groups. The upper row (A–E) represents low-magnification images (×100), whereas the lower row (F–J) shows the corresponding high-magnification images (×400). (A, F) Control group; (B, G) healthy rats treated with daidzein (DZD); (C, H) busulfan-induced premature ovarian insufficiency (POI) group; (D, I) POI treated with daidzein (POI+DZD); and (E, J) POI treated with estradiol (POI+Estr). Ovarian sections from the POI group exhibited marked depletion of developing follicles, increased follicular atresia, a substantial reduction in corpora lutea, and disruption of normal ovarian histoarchitecture. Treatment with daidzein or estradiol partially restored ovarian morphology, as evidenced by an increased number of healthy developing follicles and attenuation of follicular atresia. Arrows indicate preantral follicles. CL, corpus luteum; AF, atretic follicle; SF, secondary follicle. Scale bars: 400 µm (A–E) and 100 µm (F–J).

3.7. Hierarchical Clustering Analysis of Measured Variables

Hierarchical clustering of all measured variables identified distinct clustering patterns among the five experimental groups (Figure 5). Samples from the Control and DZD groups clustered closely, whereas samples from the POI group formed a separate cluster. The POI+DZD and POI+Estr groups exhibited clustering patterns distinct from the untreated POI group. Across variables, higher standardized values of Caspase-3 and TNF-α were observed in the POI group, whereas higher standardized values of SOD, catalase, Nrf2, FOXL2, ERα, ERβ, ovarian weight, ovarian volume, follicular counts, estradiol, and progesterone were observed in the Control, DZD, POI+DZD, and POI+Estr groups.

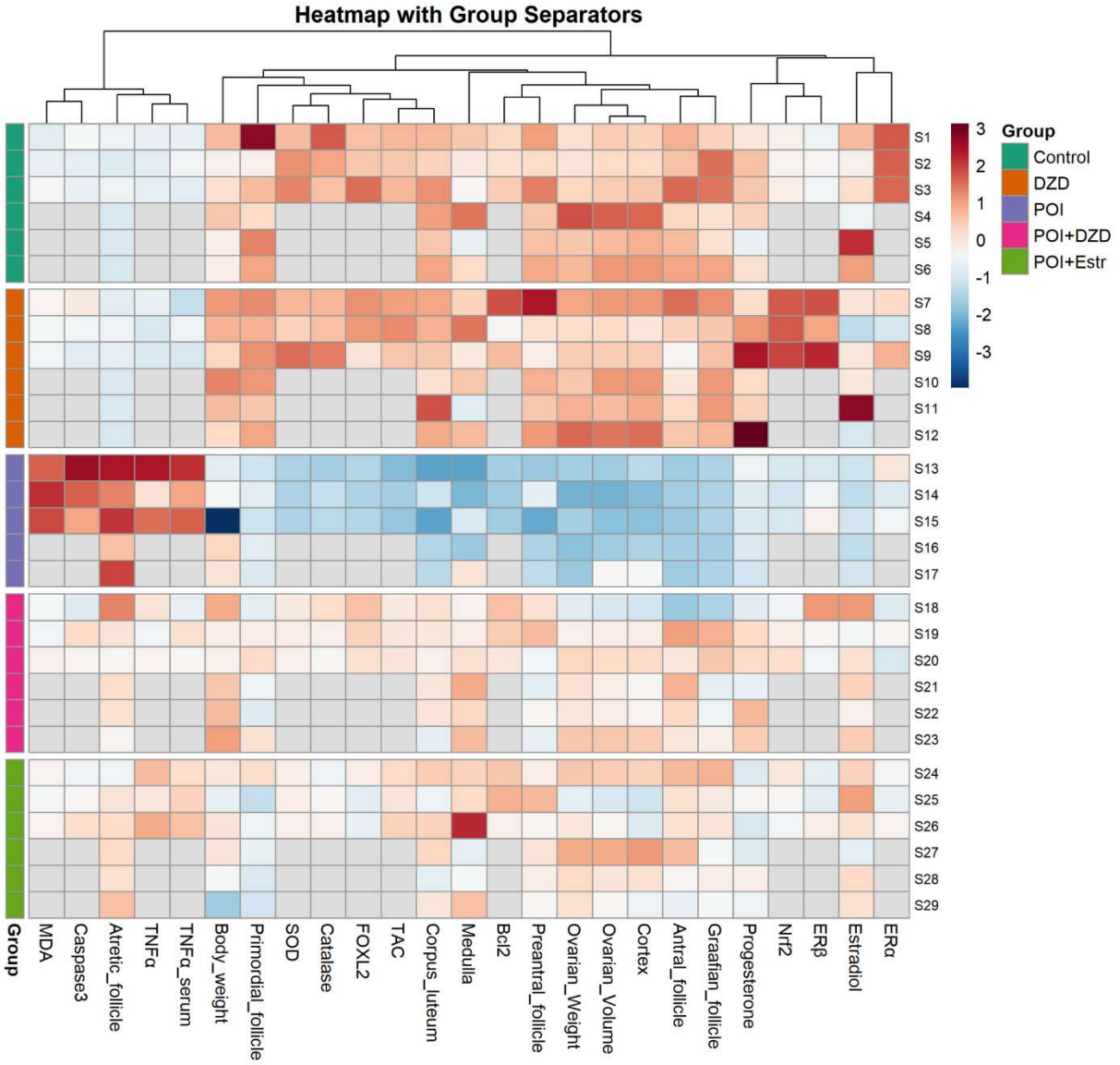


Figure 5. Hierarchical clustering heatmap illustrating the global pattern of biochemical, molecular, hormonal, stereological, and follicular parameters among the experimental groups. Color intensity represents standardized Z-scores of each variable, with red indicating relatively higher values and blue indicating lower values.

4. Discussion

This study investigated the protective effects of daidzein against busulfan-induced premature ovarian insufficiency in rats, with estradiol as a reference. Busulfan administration induced marked ovarian injury characterized by reduced ovarian weight and volume, follicle depletion across all stages, increased atresia, diminished corpus luteum volume, and disrupted steroidogenesis. These alterations were accompanied by impaired redox homeostasis (decreased SOD, CAT, TAC; increased MDA), elevated inflammation (TNF-α), and activation of intrinsic apoptosis (reduced

BCL-2, increased CASP3). Molecularly, busulfan downregulated Nrf2, FOXL2, ERα, and ERβ while upregulating TNF-α and CASP3. Daidzein significantly ameliorated these changes by restoring antioxidant capacity, suppressing inflammation and apoptosis, upregulating Nrf2 and FOXL2, and improving ovarian histoarchitecture. While estradiol exerted partial protection, daidzein demonstrated superior efficacy, suggesting its potential as a multi-target therapeutic strategy for chemotherapy-induced ovarian injury.

The significant reduction in SOD, CAT activities, and TAC, alongside elevated MDA and TNF-α in the POI group, confirms that busulfan-induced ovarian insufficiency is driven by oxidative stress and inflammatory cascades. Alkylating agents generate excessive ROS, overwhelm antioxidant defenses, and promote lipid peroxidation[25, 26]. Concurrent TNF-α elevation indicates NF-κB activation, which amplifies inflammation and sensitizes granulosa cells to apoptosis[27, 28]. This interplay forms a self-perpetuating cycle accelerating follicular depletion [29, 30].

Daidzein restored SOD, CAT activities, and TAC in the POI+DZD group, underscoring its potent antioxidant properties. As a polyphenolic isoflavone, daidzein directly scavenges ROS and enhances endogenous antioxidant enzymes [29, 31]. Consistent with the results of our study, Zhang et al showed the upregulation of Nrf2 expression in daidzein-treated animals indicates activation of the Nrf2/ARE pathway, coordinating expression of cytoprotective genes including SOD, CAT, and HO-1 [32, 33]. Notably, daidzein increased CAT activity whereas estradiol did not, suggesting antioxidant effects extend beyond estrogen receptor-mediated pathways to direct modulation of redox-sensitive transcription factors [29, 31]. The suppression of TNF-α by daidzein, but not estradiol, highlights its superior anti-inflammatory activity, likely mediated through NF-κB inhibition [28].

The significant reduction in serum estradiol and progesterone in the POI group reflects impaired steroidogenesis, consistent with follicular depletion and reduced corpus luteum formation [34, 35]. Based on the results of our study, it can be suggested. That daidzein restored both hormones, indicating partial recovery of steroidogenic capacity through: (i) ERβ-mediated phytoestrogenic activity supporting granulosa cell survival [32, 36]; (ii) preservation of follicular structures; and (iii) reduction of oxidative stress protecting steroidogenic enzymes[29, 30]. Daidzein's preferential ERβ affinity—the dominant ovarian estrogen receptor—may explain its efficacy in preserving endocrine function while minimizing systemic side effects [37, 38]. In contrast, estradiol increased serum estradiol but failed to restore progesterone, suggesting exogenous replacement does not necessarily promote luteal function[39, 40]. Despite improvements, hormone levels did not fully normalize, reflecting irreversible follicular loss and underscoring the importance of early intervention [30, 41].

Stereological analysis revealed extensive ovarian structural damage in the POI group, including reduced ovarian weight and volume, cortical and medullary volumes, corpus luteum volume, and follicle counts across all stages, with increased atresia. These findings align with previous stereological studies in chemotherapy-induced POI models [5, 30, 42]. Cortical volume reduction reflects loss of the primary follicular reservoir, while medullary reduction indicates decreased vascularization and stromal depletion [43, 44]. The increased atretic follicles confirm that busulfan promotes active follicular degeneration through apoptosis.

Daidzein and estradiol both improved stereological parameters, although complete restoration was not achieved. Daidzein's partial recovery is attributed to: (i) preservation of primordial follicles

through PI3K/Akt/FOXO3a pathway inhibition, preventing inappropriate follicular activation [45, 46]; (ii) reduced granulosa cell apoptosis via BCL-2 upregulation and CASP3 downregulation; and (iii) promotion of luteal survival through ERβ signaling and NR5A2 regulation [32, 47]. Daidzein's superior effect on preserving preantral and antral follicles suggests its antioxidant and anti-inflammatory actions are critical for maintaining follicular development beyond the primordial stage [29, 33], supported by increased FOXL2 expression in daidzein-treated animals [48, 49]. The persistent reduction in corpus luteum volume highlights luteal cell vulnerability; incomplete recovery explains persistently low progesterone levels [5, 30]. These findings emphasize that while daidzein and estradiol confer significant structural protection, they cannot fully regenerate lost follicles, reinforcing the need for fertility preservation strategies [41].

Molecular findings provide mechanistic insights. Busulfan-induced POI was characterized by downregulation of Nrf2, FOXL2, ERα, and ERβ, with upregulation of TNF-α and CASP3 and downregulation of BCL-2—reflecting convergence of oxidative stress, inflammation, and apoptosis [29, 48]. Daidzein significantly upregulated Nrf2, likely through Keap1 modification, allowing Nrf2 nuclear translocation and antioxidant gene transcription [29, 31]. Concurrent TNF-α reduction indicates NF-κB inhibition [28, 48]. BCL-2 restoration and CASP3 suppression confirm inhibition of mitochondrial apoptosis, consistent with histologically observed granulosa cell preservation.

The upregulation of FOXL2 by daidzein—whereas estradiol did not—represents a particularly important finding. FOXL2 is essential for granulosa cell differentiation, ovarian identity maintenance, and protection against oxidative stress [49]. Its downregulation following busulfan contributes to impaired folliculogenesis and accelerated atresia [50, 51]. Daidzein's ability to restore FOXL2 suggests direct modulation of granulosa cell transcriptional programs independent of estrogen receptor signaling, consistent with studies showing genistein upregulates FOXL2 through TGF-β signaling [48, 52]. Regarding estrogen receptors, daidzein increased ERβ expression in healthy animals while estradiol did not, reinforcing its role as a selective estrogen receptor modulator with preferential ERβ activity[36, 37]. However, in the POI+DZD group, ERβ remained lower than in healthy daidzein-treated animals, likely due to extensive granulosa cell loss—the primary cells expressing ERβ—suggesting that daidzein's protective effects in severe ovarian damage may be mediated more through antioxidant and anti-inflammatory actions than direct receptor modulation[31, 32].

The hierarchical clustering heatmap provides an integrated overview of the biological alterations induced by busulfan and the effects of daidzein across multiple outcome measures. The distinct clustering of the POI group from the Control and DZD groups reflects the concurrent changes in oxidative stress, inflammation, apoptosis, endocrine function, and ovarian morphology following chemotherapy-induced ovarian injury. In contrast, the clustering pattern of the POI+DZD group shifted away from the untreated POI group and was characterized by higher antioxidant, hormonal, and follicular parameters together with lower inflammatory and apoptotic markers. These findings are consistent with previous studies demonstrating that activation of the Nrf2/Keap1 antioxidant pathway and regulation of estrogen receptor signaling by daidzein contribute to the maintenance of ovarian redox homeostasis and follicular integrity under pathological conditions [36, 53, 54]. Furthermore, the positive clustering of FOXL2 with ovarian structural and hormonal parameters supports earlier reports identifying this transcription factor as a key regulator of granulosa cell function and ovarian reserve in premature ovarian insufficiency [55].

This study has several strengths: comprehensive integration of biochemical, molecular, hormonal, stereological, and histopathological assessments; use of a well-established busulfan-induced POI model; inclusion of estradiol as a positive control; and detailed mechanistic evaluation of interconnected pathways. However, limitations include: the rodent model requiring cautious extrapolation to humans; single-dose busulfan administration versus clinical fractionated regimens; evaluation of only one dose of daidzein and estradiol; a 50-day treatment duration that may not reflect long-term recovery; assessment at the mRNA level without protein confirmation; and absence of fertility outcome assessment.

Despite these limitations, daidzein—a naturally occurring compound with an established human safety profile—represents a promising adjunctive therapy for women undergoing gonadotoxic chemotherapy. Its multitarget mechanism combining antioxidant, anti-inflammatory, anti-apoptotic, and estrogenic activities offer advantages over single-target interventions. However, given incomplete restoration of ovarian reserve, daidzein should be considered complementary to established fertility preservation methods such as oocyte or embryo cryopreservation (36,56). Future research should optimize dosing regimens, evaluate combination therapies, and assess long-term effects on fertility and offspring health.

5. Conclusion

In conclusion, this study demonstrates that daidzein exerts significant protective effects against busulfan-induced POI through multiple mechanisms: (i) restoration of redox homeostasis via Nrf2-mediated upregulation of antioxidant enzymes; (ii) suppression of inflammation through TNF-α inhibition; (iii) inhibition of mitochondrial apoptosis by upregulating BCL-2 and downregulating CASP3; (iv) preservation of granulosa cell function through FOXL2 upregulation; and (v) modulation of estrogen receptor signaling, particularly ERβ, supporting follicular survival and steroidogenesis. While estradiol provided partial protection, daidzein demonstrated superior efficacy in preserving ovarian structure, follicular reserve, and steroidogenic function, likely due to its combined phytoestrogenic and antioxidant properties. However, incomplete restoration to control levels underscores the irreversible nature of some chemotherapy-induced damage and highlights the need for early intervention and combination with fertility preservation strategies. These findings support daidzein as a promising natural therapeutic candidate for mitigating ovarian toxicity in patients undergoing gonadotoxic chemotherapy, warranting further preclinical and clinical investigation.

Declarations

Ethics approval

All animal experiments adhere to the ARRIVE standards and are conducted in accordance with the UK Animals (Scientific Procedures) Act, 1986, as well as the EU Directive 2010/63/EU regarding animal experimentation. This study was approved locally by the Ethics Committee of Shiraz University of Medical Sciences (Code: IR.SUMS.AEC.1402.074).

Consent for publication

Not applicable.

Availability of data and materials

This article contains all data created and examined throughout this investigation. The corresponding author will provide datasets used or analyzed during the current work upon reasonable request.

Competing interests

On behalf of all authors, the corresponding author states that there is no conflict of interest.

Funding

The present article was extracted from the thesis written by Fatemeh Rahimi has been submitted in Shiraz University of Medical Sciences, Shiraz, Iran. [grant number: 32812].

Authors' Contributions

Conceptualization and study design: F.Rahimi
Methodology and investigation:
Formal analysis and data curation:
Writing – review & editing:
Supervision and project administration:
Final manuscript approval: All authors have read, revised, and approved the final version of the manuscript.

Acknowledgments

References:

1. Guo, T., et al., *Epidemiology, genetic etiology, and intervention of premature ovarian insufficiency.* Endocrine Reviews, 2025. **46**(5): p. 621-651.
2. Golezar, S., et al., *The global prevalence of primary ovarian insufficiency and early menopause: a meta-analysis.* Climacteric, 2019. **22**(4): p. 403-411.
3. Foster, K.L., et al., *Ovarian insufficiency and fertility preservation during and after childhood cancer treatment.* Journal of Adolescent and Young Adult Oncology, 2024. **13**(3): p. 377-388.
4. Zhao, P., et al., *Chemotherapy-induced ovarian damage and protective strategies.* Human Fertility, 2023. **26**(4): p. 887-900.
5. Li, X., et al., *Immunity and reproduction protective effects of Chitosan Oligosaccharides in Cyclophosphamide/Busulfan-induced premature ovarian failure model mice.* Frontiers in immunology, 2023. **14**: p. 1185921.
6. Jiang, Y., et al., *Accelerated ovarian aging in mice by treatment of busulfan and cyclophosphamide.* Journal of Zhejiang University Science B, 2013. **14**(4): p. 318-324.
7. Yan, F., et al., *The role of oxidative stress in ovarian aging: a review.* J Ovarian Res, 2022. **15**(1): p. 100.
8. Gao, X., et al., *Role of the Nrf2 Signaling Pathway in Ovarian Aging: Potential Mechanism and Protective Strategies.* Int J Mol Sci, 2023. **24**(17).
9. Pisarska, M.D., G. Barlow, and F.T. Kuo, *Minireview: roles of the forkhead transcription factor FOXL2 in granulosa cell biology and pathology.* Endocrinology, 2011. **152**(4): p. 1199-208.

10. Zhang, Y., et al., *Regulation of FOXL2 gene in ovarian granulosa cell tumor by JNK inhibitor.* Sci Rep, 2025. **15**(1): p. 12167.
11. Ju, W., et al., *Mitochondria-driven inflammation: a new frontier in ovarian ageing.* J Transl Med, 2025. **23**(1): p. 1005.
12. Zhang, S., et al., *The Impact of Oxidative Stress Imbalance on Ovarian Function and Its Mechanisms.* Int J Gen Med, 2026. **19**: p. 616217.
13. Jia, C., et al., *Mechanisms of mitochondrial dysfunction in premature ovarian insufficiency.* Journal of Ovarian Research, 2026.
14. Bao, X., et al., *Role of ERβ in the ovary and ovary related diseases.* Gene, 2024. **927**: p. 148678.
15. Dinh, D.T., et al., *Estrogen receptor alpha and beta chromatin interactions govern ovarian folliculogenesis but dissipate during ovulation.* Endocrinology, 2026. **167**(6): p. bqag052.
16. Alshehri, M.M., et al., *Therapeutic Potential of Isoflavones with an Emphasis on Daidzein.* Oxid Med Cell Longev, 2021. **2021**: p. 6331630.
17. Intharuksa, A., et al., *Daidzein and Genistein: Natural Phytoestrogens with Potential Applications in Hormone Replacement Therapy.* Int J Mol Sci, 2025. **26**(14).
18. Xie, K., et al., *Daidzein supplementation improved fecundity in sows via modulation of ovarian oxidative stress and inflammation.* J Nutr Biochem, 2022. **110**: p. 109145.
19. Karp, N.A., et al., *Applying the ARRIVE guidelines to an in vivo database.* PLoS biology, 2015. **13**(5): p. e1002151.
20. Manshadi, M.D., et al., *The effects of human menstrual blood stem cells-derived granulosa cells on ovarian follicle formation in a rat model of premature ovarian failure.* Microsc Res Tech, 2019. **82**(6): p. 635-642.
21. Laddha, A.P. and Y.A. Kulkarni, *Daidzein ameliorates peripheral neuropathy in Sprague Dawley rats.* Front Pharmacol, 2024. **15**: p. 1385419.
22. Neisy, A., et al., *Daidzein improves neuronal health and alleviates inflammation and apoptosis through BDNF and estrogen receptors in the hippocampus of ovariectomized rats.* Iran J Basic Med Sci, 2025. **28**(7): p. 888-898.
23. Noorafshan, A., et al., *Stereological study of the effects of letrozole and estradiol valerate treatment on the ovary of rats.* Clin Exp Reprod Med, 2013. **40**(3): p. 115-21.
24. Vakili, S., et al., *The Effects of L-Tartaric Acid on Ovarian Histostereological and Serum Hormonal Analysis in an Animal Model of Polycystic Ovary Syndrome.* Reprod Sci, 2024. **31**(11): p. 3583-3594.
25. Chen, J., et al., *Pharmacological effects and mechanisms of medicine food homology species and active ingredients in ameliorating ovarian aging.* Frontiers in Nutrition, 2026. **12**: p. 1756703.
26. Trujillo, M., et al., *Chemotherapy induced oxidative stress in the ovary: drug-dependent mechanisms and potential interventions.* Biology of Reproduction, 2023. **108**(4): p. 522-537.
27. Dutta, S., et al., *Targeting Polycystic Ovary Syndrome (PCOS) Pathophysiology with Flavonoids: From Adipokine-Cytokine Crosstalk to Insulin Resistance and Reproductive Dysfunctions.* Pharmaceuticals (Basel), 2025. **18**(10).
28. Kim, J.W., et al., *Daidzein administration in vivo reduces myocardial injury in a rat ischemia/reperfusion model by inhibiting NF-kappaB activation.* Life Sci, 2009. **84**(7-8): p. 227-34.
29. Shi, Y.-Q., et al., *Premature ovarian insufficiency: a review on the role of oxidative stress and the application of antioxidants.* Frontiers in endocrinology, 2023. **14**: p. 1172481.
30. Hao, X., et al., *Ovarian follicle depletion induced by chemotherapy and the investigational stages of potential fertility-protective treatments—a review.* International journal of molecular sciences, 2019. **20**(19): p. 4720.
31. Rimbach, G., et al., *Antioxidant and free radical scavenging activity of isoflavone metabolites.* Xenobiotica, 2003. **33**(9): p. 913-925.

32. Zhang, Q., et al., *Effects of dietary daidzein supplementation on reproductive performance, serum hormones, and reproductive-related genes in rats.* Nutrients, 2018. **10**(6): p. 766.
33. Peng, Y., et al., *Berberine protects cyclophosphamide and busulfan-induced premature ovarian insufficiency in mouse model.* Journal of Pharmacological Sciences, 2023. **153**(1): p. 46-54.
34. POI, E.G.G.o., et al., *ESHRE Guideline: management of women with premature ovarian insufficiency.* Human reproduction, 2016. **31**(5): p. 926-937.
35. Torrealday, S., P. Kodaman, and L. Pal, *Premature Ovarian Insufficiency-an update on recent advances in understanding and management.* F1000Research, 2017. **6**: p. 2069.
36. Nynca, A., et al., *Effects of phytoestrogen daidzein and estradiol on steroidogenesis and expression of estrogen receptors in porcine luteinized granulosa cells from large follicles.* Acta physiologica Polonica, 2009. **60**(2): p. 95.
37. Kuiper, G.G., et al., *Interaction of estrogenic chemicals and phytoestrogens with estrogen receptor beta.* Endocrinology, 1998. **139**(10): p. 4252-63.
38. Moutsatsou, P., *The spectrum of phytoestrogens in nature: our knowledge is expanding.* Hormones (Athens), 2007. **6**(3): p. 173-93.
39. Wang, Z., et al., *Exogenous estrogen partially rescues progesterone deficiency and autophagosome enlargement in Mcoln1-/-mouse model with lysosomal storage disorder.* Reproductive and Developmental Medicine, 2024. **8**(04): p. 197-205.
40. Mauvais-Jarvis, F., D.J. Clegg, and A.L. Hevener, *The role of estrogens in control of energy balance and glucose homeostasis.* Endocrine reviews, 2013. **34**(3): p. 309.
41. Spears, N., et al., *Ovarian damage from chemotherapy and current approaches to its protection.* Hum Reprod Update, 2019. **25**(6): p. 673-693.
42. Morgan, S., et al., *How do chemotherapeutic agents damage the ovary?* Hum Reprod Update, 2012. **18**(5): p. 525-35.
43. Soleimani, R., et al., *Mechanisms of chemotherapy-induced human ovarian aging: double strand DNA breaks and microvascular compromise.* Aging (Albany NY), 2011. **3**(8): p. 782-93.
44. Meirow, D., et al., *Cortical fibrosis and blood-vessels damage in human ovaries exposed to chemotherapy. Potential mechanisms of ovarian injury.* Hum Reprod, 2007. **22**(6): p. 1626-33.
45. Li, J., et al., *Quercetin prevents primordial follicle loss via suppression of PI3K/Akt/Foxo3a pathway activation in cyclophosphamide-treated mice.* Reprod Biol Endocrinol, 2021. **19**(1): p. 63.
46. Chang, E.M., et al., *Cisplatin Induces Overactivation of the Dormant Primordial Follicle through PTEN/AKT/FOXO3a Pathway which Leads to Loss of Ovarian Reserve in Mice.* PLoS One, 2015. **10**(12): p. e0144245.
47. Bertolin, K., et al., *The orphan nuclear receptor Nr5a2 is essential for luteinization in the female mouse ovary.* Endocrinology, 2014. **155**(5): p. 1931-43.
48. Haddad, Y.H., et al., *Phytoestrogen genistein hinders ovarian oxidative damage and apoptotic cell death-induced by ionizing radiation: co-operative role of ER-β, TGF-β, and FOXL-2.* Scientific Reports, 2020. **10**(1): p. 13551.
49. Benayoun, B.A., et al., *Transcription factor FOXL2 protects granulosa cells from stress and delays cell cycle: role of its regulation by the SIRT1 deacetylase.* Hum Mol Genet, 2011. **20**(9): p. 1673-86.
50. Uda, M., et al., *Foxl2 disruption causes mouse ovarian failure by pervasive blockage of follicle development.* Hum Mol Genet, 2004. **13**(11): p. 1171-81.
51. Schmidt, D., et al., *The murine winged-helix transcription factor Foxl2 is required for granulosa cell differentiation and ovary maintenance.* Development, 2004. **131**(4): p. 933-42.
52. Marcozzi, S., et al., *Distinct effects of epirubicin, cisplatin and cyclophosphamide on ovarian somatic cells of prepuberal ovaries.* Aging (Albany NY), 2019. **11**(22): p. 10532-10556.
53. Zhang, S., et al., *Chemotherapy impairs ovarian function through excessive ROS-induced ferroptosis.* Cell Death Dis, 2023. **14**(5): p. 340.

54. Zhang, T., et al., *Mechanisms of primordial follicle activation and new pregnancy opportunity for premature ovarian failure patients.* Front Physiol, 2023. **14**: p. 1113684.
55. Thanatsis, N., et al., *Reduced Foxo3a, FoxL2, and p27 mRNA expression in human ovarian tissue in premature ovarian insufficiency.* Hormones (Athens), 2019. **18**(4): p. 409-415.